Exercise Monitoring and Assessment System for Home-Based Respiratory Rehabilitation

Dou Fan, Xiaodong Yang, *Senior Member, IEEE*, Nan Zhao and Lei Guan, Qammer H. Abbasi, *Senior Member, IEEE*

***Abstract*—Exercise training is a key component of respiratory rehabilitation. Exercise monitoring and assessment have shown to be beneficial and have significant improvement in the outcome of exercise training. In this paper, we propose a non-invasive exercise monitoring and assessment system (EMAS) to home-based respiratory rehabilitation exercises. EMAS exploits multi-band microwave sensing technique to monitor in real-time the patient's rehabilitation exercise training, and synchronously provide an online visual feedback for helping the patient better training. Then EMAS extracts exercise information (duration, intensity and breathing changes) from all exercise data to assess the quality of rehabilitation exercise. We implement EMAS on the designed compact and portable prototypes and deploy it to monitor 4 subjects, resulting in one week of exercise data in total. System evaluations demonstrate that EMAS can accurately monitor rehabilitation exercises of each subject and obtain the exercise duration, exercise intensity and breathing changes during rehabilitation exercises to achieve exercise assessment.**

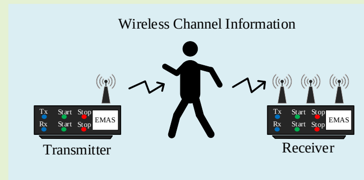

***Index Terms*—Exercise monitoring, respiratory rehabilitation, home therapy, multi-band microwave sensing**

I. Introduction

RESPIRATORY rehabilitation, also called pulmonary rehabilitation, is an evidence-based, multidisciplinary, conventional and comprehensive intervention for patients with chronic respiratory diseases. Respiratory rehabilitation is the use of exercise, education, and behavioral intervention to improve the physical and psychological condition of people with chronic respiratory diseases [1]. Numerous studies on evidence-based medicine have shown that pulmonary rehabilitation centered on exercise therapy is beneficial to patients with respiratory diseases. The benefits include significantly improved exercise endurance [2], enhanced respiratory muscle function and reduced dyspnea [3], improved health-related quality of life [4], and relieved disease-related anxiety and depression [5]. Thus, early intervention and continuous availability of pulmonary rehabilitation services are crucial for patients with respiratory diseases. On the other hand, the current global pandemic of coronavirus disease 2019 (COVID-19) is a serious respiratory disease, which can cause lung damage and breathing problems. The most commonly reported symptoms of patients with COVID-19 infection involve the respiratory tract. Such clinical respiratory symptoms include fever, cough, fatigue and dyspnea, and some severe patients gradually develop crippling symptoms like respiratory failure, septic shock, and/or multiple organ dysfunction/failure [6-8]. Pulmonary rehabilitation may relive the symptoms associated with COVID-19, increase the cardiopulmonary endurance, and improve physical and mental health, which is favorable for patients to recovery and return to society.

Exercise training is the most important component of pulmonary rehabilitation and is significant for the marked improve lung function. Monitoring exercise training not only helps patients keep track of their physical healthy condition, but also allows doctors to have a clear view of their patient's rehabilitation progress and to carry on reasonable instruction. At present, most patients need the specialized physiotherapist to assist with rehabilitation exercise training, thereby increasing cost of treatment for the patient and heavy workload for the specialized physiotherapist. To solve this problem, many methods have been proposed to monitor rehabilitation exercises, mainly including *sensor-based*, *vision-based*, and *RF-based*.

Sensor-based rehabilitation exercise monitoring. Inertial measurement units (IMU) are the sensor most commonly used in this category. The IMU measures acceleration, angular velocity, and magnetic field strength using a combination of accelerometers, gyroscopes, and magnetometers [9]. Using IMU for monitoring rehabilitation exercise has attracted much research attention and has gained many achievements. Inertial sensor is used to monitor and evaluate rehabilitation exercises for shoulder [10, 11], upper limb [12, 13], and lower limb exercises [14]. These works demonstrated the feasibility of using inertial sensor for rehabilitation exercise monitoring and

The work was supported by the Key Research and Development Program of Shaanxi (Program No. 2022KW-44), National Natural Science Foundation of China (Grant No. 61671349), Innovation Capability Support Program of Shaanxi (Program No. 2021TD-07).

Dou Fan is with the School of Life Science and Technology, Xidian University, Xi'an, Shaanxi, China, 710126.

Xiaodong Yang, Nan Zhao, Lei Guan are with the Key Laboratory of High Speed Circuit Design and EMC, Ministry of Education, School of Electronic Engineering, Xidian University, Xi'an, Shaanxi, China, 710071.

Qammer H. Abbasi is with the James Watt School of Engineering, University of Glasgow, UK, G12 8QQ.

Corresponding authors: Xiaodong Yang, Nan Zhao.

recognition. In addition, other kinds of sensors are also used to monitor and improve rehabilitation exercises. For example, electromyography (EMG) sensor can provide significant motion-related information for rehabilitation exercises [15]. However, these methods require users to wear sensors, making their life inconvenient, and it is unfriendly for the disabled and the elderly to wear sensors. Moreover, such methods also fail to provide visual feedback to users.

Vision-based rehabilitation exercise monitoring. Kinect, due to its low-cost and convenient operation, is widely used for monitoring rehabilitation exercises. Kinect is a composite device that contains an infrared (IR) projector, an IR camera and a color (RGB) camera [16]. Some studies have validated the capability of Kinect as a marker-less motion tracking device for rehabilitation exercises monitoring [17-20]. These systems capture the user's motions using the Kinect and provide a visual feedback during exercise sessions. Nevertheless, the occlusion problem and limited sensing range limit the application of vision-based methods in rehabilitation exercises.

RF-based rehabilitation exercise monitoring. With the fast development of wireless communication, radiofrequency (RF)-based methods are becoming a promising alternative of human motion sensing. Since the method is not susceptible to the light and temperature and privacy-friendly without physical contacts and leaking the person's appearance and sound, many RF-based human motion sensing methods have been proposed. For example, RF-Wri [21] recognizes the air-written letters using the USRP-B210 hardware. RF-Pose3D [22] leverages custom-designed Frequency Modulated Carrier Wave (FMCW) to track 3D human skeletons and their movements. Soli [23] is designed for fine-grained hand gestures recognition and tracking based on millimeter-wave (mmWave) radar. Due to the need for specialized hardware, these methods have significant limitations. In comparison, WiFi-based sensing method is an emerging potential solution for human motion sensing due to the ubiquitous nature of WiFi in everyday life. WiFi-based human motion sensing has made great effort focusing on several application areas such as indoor localization [24, 25], activity recognition [26-28], fine-grained motion sensing [29, 30], health monitoring [31-33]. Some recent studies have further confirmed that WiFi-based human motion sensing method has promising applications in recognizing daily activities. For instance, the authors in [34] presented a multimodal fusion-AdaBoost based human activity recognition scheme to recognize six common daily activities (walking, running, sitting, lying, standing, and falling) using WiFi signals. The work [35] proposed a Multilayer Bi-directional Long Short-Term Memory framework for contactless real-time activity detection by exploiting WiFi Channel State Information data. The researchers in [36] designed an Augment Few Shot Learning-based Human Activity Recognition (AFSL-HAR) system based on WiFi Channel State Information.

Although previous researches by WiFi-based sensing method have achieved great achievements, few efforts have been made on rehabilitation exercise monitoring, a noteworthy field. Moreover, in the context of COVID-19, Home-based respiratory rehabilitation exercises are conducive to recover physical health for discharged patients with COVID-19. Motivated by these findings, our work turns to rehabilitation exercise monitoring based on WiFi sensing. WiFi-based sensing method can be well applied in rehabilitation exercise monitoring because of its low cost, unobtrusive characteristics and robust sensing capabilities.

In this paper, we propose an exercise monitoring and assessment system, named EMAS, to monitor in real-time and assess home-based respiratory rehabilitation exercise training using WiFi-based multi-band microwave sensing technique. EMAS works in a non-invasive manner without any body contact. We first exploit multi-band microwave sensing technique to monitor the exercise training in pulmonary rehabilitation and collect the corresponding data. Meanwhile, these data are preprocessed and synchronously displayed in a graphical form, provided a visual feedback for the patient to help the patient better training. Next, all collected data need to go through further analyzing to extract useful information. We then assess this information and feedback the results to the patient and doctors. By experimental verification, EMAS can not only accurately monitor patients' exercise training but also extract exercise information to assess the effect of rehabilitation training.

It is important to note that this paper does not introduce a new rehabilitation exercise training, but proposes a new solution for non-contact monitoring and assessment rehabilitation exercise training using multi-band microwave sensing technique. The system components involved in this study have already proved to be able to accurately and reliably monitor and evaluate rehabilitation exercise training.

In summary, the main contributions of this paper are as follows:

- A non-contact exercise monitoring and assessment system (EMAS) is proposed, which not only can monitor patient performance in real-time but also can provide exercise assessment to understand the patient's rehabilitation effect.
- A real-time visual feedback is presented for patients' home-based rehabilitation exercise training without violating the patient's privacy, so as to help them better complete exercise training.
- A compact and portable prototype of EMAS is designed and we conduct extensive experiments using it. Results illustrate that EMAS is effective for monitoring and assessment the quality of home-based rehabilitation exercise training.

The rest of the paper is organized as follows. Section II introduces the preliminaries of multi-band microwave sensing technique. Section III introduces the taxonomy of rehabilitation exercises and the overall workflow of EMAS, and Section IV describes the detail system design. Section V presents the experimental evaluation of EMAS. Finally, Section VI concludes the paper.

II. Preliminaries

In this section, we introduce the technical background of multi-band microwave sensing technique, including the wireless channel information (WCI) and the impact of human motion on the variations of WCI from the mathematical point of view.

A. Wireless Channel Information

EMAS uses multi-band microwave sensing technique that operates at S-band and C-band. The technique combines Orthogonal Frequency Division Multiplexing (OFDM) and multiple-input multiple-output (MIMO). The multi-band microwave sensing technique continuously monitors wireless channel variations using wireless channel information. The WCI uses the channel frequency response (CFR) to describe channel characteristics. Let $X(f,t)$ be the frequency domain representations of transmitted signals, thus the received signals are expressed as

$$Y(f,t)=H(f,t)\times X(f,t) \tag{1}$$

where $H(f,t)$ is the complex-valued CFR at frequency f and time t. If the wireless link has N_t and N_r transmitting and receiving antennas respectively, and for each pair of transmitting and receiving antenna WCI is measured on 30 selected OFDM subcarriers, so each WCI measurement is a struct with dimensions $N_t \times N_r \times 30$. Each term in the struct is a CFR value between a pair of antennas at a certain subcarrier frequency at a particular time. The CFR value is also called as the WCI value.

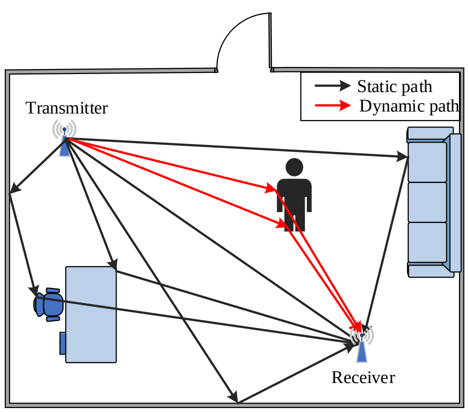

Fig. 1. Multipath propagation.

B. Wireless Channel Analysis

In indoor environments, wireless signals arrive at the receiver from the transmitter through multiple paths including the line of sight (LoS) path, static paths reflected by surrounding objects and dynamic paths reflected by human motion, as illustrated in Fig. 1. Assuming a wireless signal arrives at the received antenna of a given antenna pair through N different paths, then $H(f,t)$ is generally modeled as

$$H(f,t)=\sum_{i=1}^{N} a_i(f,t)e^{-j2\pi f\tau_i(t)} \tag{2}$$

where $a_i(f,t)$ is the complex amplitude of the i^{th} path, $e^{-j2\pi f\tau_i(t)}$ is the phase shift of the i^{th} path on the propagation delay $\tau_i(t)$. Actually, the wireless channel information has non-negligible phase shift because of the imperfect synchronization between the transmitter and receiver in analog/digital domains. So $H(f,t)$ is written as

$$H(f,t)=e^{-j\theta(t)}\sum_{i=1}^{N} a_i(f,t)e^{-j2\pi f\tau_i(t)} \tag{3}$$

where $e^{-j\theta(t)}$ denotes the phase shift caused by symbol timing offset (STO), sampling frequency offset (SFO), carrier frequency offset (CFO), and carrier phase offset (CPO) [37].

Human motion can lead to the changes in the propagation path. As shown in Fig. 2(a), when the human body moves a small distance from time 0 to time t, the propagation distance of the i^{th} path reflected by the human body changes from $d_i(0)$ to $d_i(t)$. The propagation delay is the function of the propagation distance: $\tau_i(t)=d_i(t)/c$, where c is the velocity of electromagnetic wave propagation in free space and $d_i(t)$ is the propagation distance of the i^{th} path. The relationship between the wavelength and the frequency of an electromagnetic is given as $\lambda=c/f$. Thus, $e^{-j2\pi f\tau_i(t)}$ can be written as $e^{-j2\pi d_i(t)/\lambda}$. When the human body is within range of the wireless signal, the propagation path can be regarded as a sum of static multipath components and dynamic multipath components as shown in Fig. 2(a). Let P_s and P_d be the set of static paths and dynamic paths respectively, then $H(f,t)$ is further expressed as

$$\begin{aligned} H(f,t) &= e^{-j\theta(t)}\Big(\sum_{l\in P_s} a_l(f)e^{-\frac{j2\pi d_l}{\lambda}} + \sum_{k\in P_d} a_k(f,t)e^{-\frac{j2\pi d_k(t)}{\lambda}}\Big) \\ &\triangleq e^{-j\theta(t)}(H_s(f)+H_d(f,t)) \end{aligned} \tag{4}$$

here, $H_s(f)$ is the sum of CFR for static multipath components, $H_d(f,t)$ is the sum of CFR for dynamic multipath components whose distance change with human movements. The total CFR $H(f,t)$ is time-varying because it is the linear superposition of a constant vector $H_s(f)$ and a dynamic vector with time-varying phases and amplitudes, as shown in Fig. 2(b).

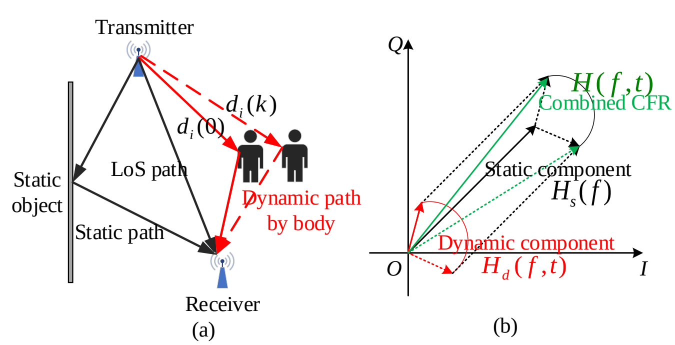

Fig. 2. Signal variation caused by human motion.

The raw phase information is randomly distributed and not available due to influence of the random phase shift $e^{-j\theta(t)}$, but the CFR power $|H(f,t)|^2$ is not affected by the phase shift, and can retain the changes of the received signal caused by human motion, the reason is as follows

$$\begin{aligned} |H(f,t)|^2 &= \left|e^{-j\theta(t)}(H_s(f)+H_d(f,t))\right|^2 \\ &= \left|H_s(f)+\sum_{k\in P_d} a_k(f,t)e^{-\frac{j2\pi d_k(t)}{\lambda}}\right|^2 \\ &= |H_s(f)|^2+\sum_{k\in P_d}|a_k(f,t)|^2 \\ &+\sum_{k\in P_d} 2|H_s(f)a_k(f,t)|\cos\left(\frac{2\pi d_k(t)}{\lambda}+\phi_{lk}\right) \end{aligned} \tag{5}$$

where $|H(f,t)|^2$ represents the instantaneous CFR power at time t. ϕ_{lk} is constant value representing initial phase shift between the static signal and the dynamic signal. Equation (5) provides two key points: 1) the CFR power can be used to sense human motion, which varies with the propagation distance of the reflected signal caused by human motion; 2) the time series CFR power goes up and down like a sinusoidal wave when the reflected path is changed by human motion. When the propagation distance of the reflected signal changes by λ, the CFR power yields a cycle of cosine wave, and when the variation of the propagation distance is less than λ, the CFR power corresponds to a fragment of cosine wave cycle.

For these reasons, the amplitude information (the square root of the CFR power) is used to monitor human motion. Specifically, each received WCI value contains the amplitude and phase information of a single subcarrier

$$H(f_i,t)=\|H(f_i,t)\|e^{-j\angle H(f_i,t)} \tag{6}$$

where $\|H(f_i,t)\|$ and $\angle H(f_i,t)$ are the amplitude information and phase information of the i^{th} subcarrier, respectively.

III. Overview

This section introduces the taxonomy of the selected rehabilitation exercises and the overall workflow of EMAS.

A. Taxonomy of Rehabilitation Exercises

Based on pulmonary rehabilitation guidelines for patients with respiratory diseases, pulmonary rehabilitation recommendations mostly include aerobic exercise, strength training, and breathing exercises [38, 39]. Therefore, in this paper we choose three kinds of rehabilitation exercise: aerobic exercise, strength training and breathing exercises, and these exercises we select that is easy to do at home and can be done independently. Concretely, aerobic exercise includes brisk walking and stair climbing, strength training includes dumbbell front raise and dumbbell lateral raise, and breathing exercises include abdominal breathing (also called diaphragmatic breathing or belly breathing) and pursed-lip breathing, their motion diagram are given in Fig. 3.

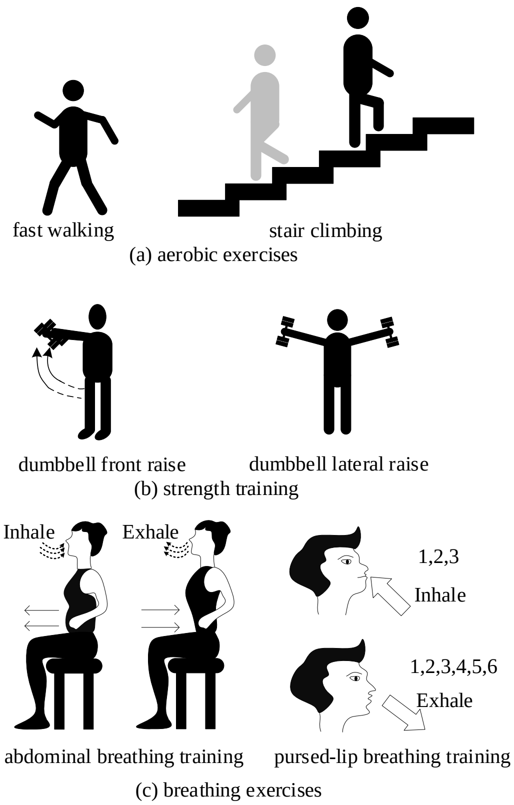

Fig. 3. The motion diagram of (a) aerobic exercises, (b) strength training, and (c) breathing exercises.

1) *Aerobic Exercises*

Brisk walking and stair climbing are simple and available aerobic exercises and easy to fit into our daily routine. For aerobic exercise, the exercise program starts from a low intensity and gradually increasing the intensity and duration, 20-30 min each time, 3-5 times a week [38]. The patient can perform exercise program at the right intensity based on his or her own physical conditions. In this paper, we propose a 30-minute exercise program of brisk walking and a 30-minute exercise program of stair climbing, as Fig. 4 shows.

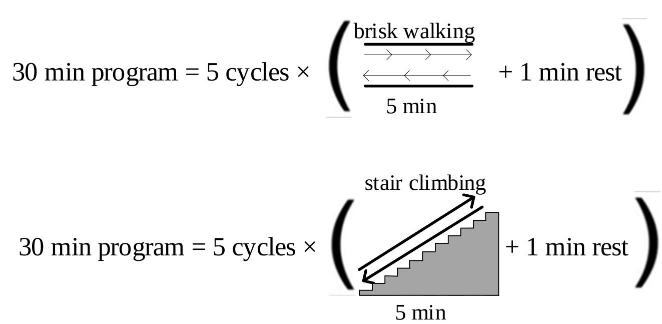

Fig. 4. Schematic representation of a brisk-walking exercise program and a stair-climbing exercise program.

2) *Strength Training*

Strength training is a valuable adjunct to dynamic exercise rehabilitation. Using sandbags, dumbbells, elastic bands or bottled water do resistance training to increase strength. The dumbbell front raise and the dumbbell lateral raise are simple and fundamental strength training. Progressive resistance training is recommended for strength training, with 15-20 movements each set with 1-2 sets each time for 3-5 times per week [39]. In accordance with this principle, we design an exercise program for strength training, as shown in Fig. 5.

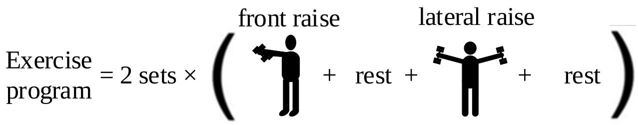

Fig. 5. Schematic representation of a strength-training exercise program.

3) *Breathing Exercises*

Breathing exercises can improve pulmonary function and improve breathing efficiency. Abdominal breathing and pursed-lip breathing are popular forms of breathing exercises. Abdominal breathing (also called diaphragmatic breathing or belly breathing) is a type of breathing exercises that helps strengthen your diaphragm, a very important muscle that encourages full oxygen exchange [40]. Pursed-lip breathing is a breathing technique that allows the control of oxygenation and ventilation. The technique requires an individual to inspire through the nose and exhale through the mouth at a slow controlled flow [41]. Breathing exercises should be practice multiple times a day with 5-10 minutes each time, and patients adjust the intensity based on their own condition.

B. System Overview

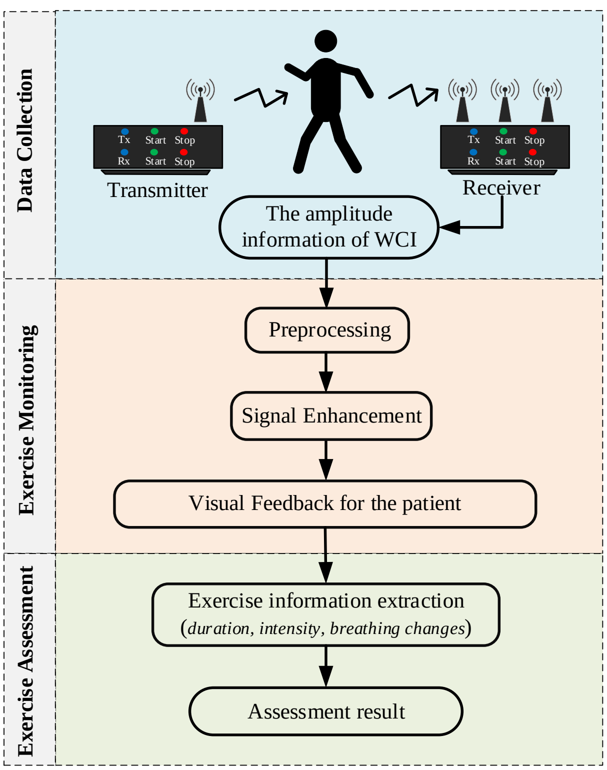

Fig. 6. System Overview.

EMAS exploits multi-band microwave sensing that its core idea is to sense human body movements through capturing wireless signals of surrounding environment. The architecture of EMAS is illustrated in Fig. 6. It mainly consists of three modules: Data Collection, Exercise Monitoring, and Exercise Assessment. The Data Collection module collects wireless signals using the designed compact and portable prototype. The Exercise Monitoring module includes preprocessing, signal enhancement and visual feedback for the patient. We use the Hampel identifier for preprocessing and combines subcarriers in an optimal way using Maximal Ratio Combining (MRC). After that, the data of each exercise are displayed in real time to provide visual feedback for the patient. The Exercise Assessment module includes exercise information extraction and assessment result, and these results are used to measure the effect of rehabilitation exercise training and are fed back to the patient and doctors.

IV. System Design

This section details the design of EMAS and highlights the key techniques behind the rehabilitation exercise monitoring and assessment.

A. Data Collection

The EMAS collects WCI measurements using a pair of compact and portable prototypes with size 127 mm × 200 mm × 75 mm, as shown in Fig. 7. The transmitter is equipped with one antenna and the receiver has three antennas. For each pair of transmitting and receiving antenna, WCI can be acquired from 30 OFDM subcarriers. So each WCI measurement contains a total of $1\times3\times30$ WCI values. When the sampling rate is 50 Hz, there are 90×50 WCI values in one second. We then extract the amplitude information from these WCI values. In this paper, EMAS takes as input time-series WCI amplitude measurements.

Fig. 7. The prototype of EMAS.

B. Exercise Monitoring

Due to the influence of environmental noise, there are some outliers of amplitude information in the collected WCI measurements. To improve system accuracy, these outliers must be eliminated. We apply the Hampel identifier [42] at each

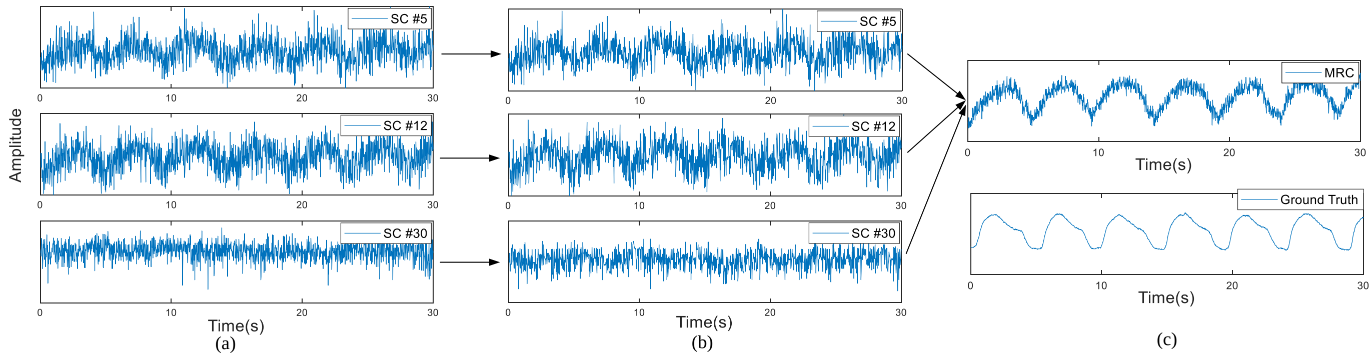

Fig. 9. Example of MRC method for optimal subcarrier combining. (a) raw breathing signal with different SNRs, (b) breathing signal after removing outliers by the Hampel filter, (c) breathing signal after using MRC.

subcarrier to detect and remove outliers. The Hampel identifier is a variation of the three-sigma rule, which uses the median and median absolute deviation to identify effectively the outliers.

To enhance the motion features at the maximum level, we propose a novel method based on Maximal Ratio Combining (MRC) to combine optimally all subcarriers. MRC is a diversity combining technique in telecommunications that maximizes SNR by combining signals from each branch or channel [43]. MRC is applicable to subcarrier combination by regarding WCI amplitudes of 90 subcarriers from three receiving antennas as the receiving diversity. The method of applying MRC for optimal subcarrier combining is shown in Fig. 8. Here we take respiratory signals as an example to illustrate the superiority of the proposed MRC-based method. The reason is that minute respiratory motions are easily overwhelmed in noise compared to other rehabilitation exercise motions.

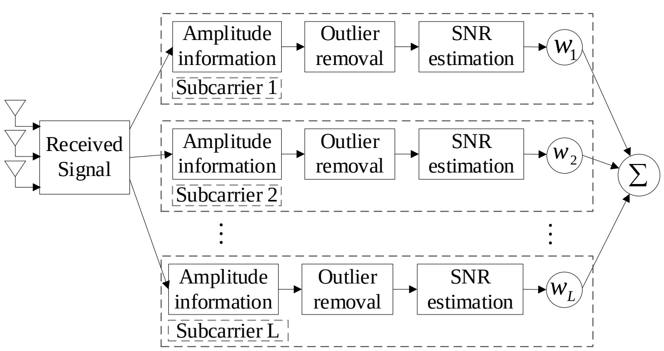

Fig. 8. The diagram of applying MRC for optimal subcarrier combining.

For the received breathing signal, the WCI amplitude of each subcarrier is a combination of breathing signal and noise. The SNR of each subcarrier is different because different subcarriers have different sensitivity to chest and abdominal movement caused by breathing, which is reflected in the respiration waveform are the respiratory movement causes different extents of signal fluctuation on different subcarriers, as illustrated in Fig. 9(a).

MRC can combine subcarriers with different SNR by providing the weight of each subcarrier, and the weight ratio of each subcarrier is equal to the channel gain ratio of its subcarriers. The channel gain of each subcarrier is proportional to the SNR in that subcarrier. In other words, the larger the SNR, the greater the weight, and hence more contribution to the combined signal. Therefore, we first compute the SNR of each subcarrier. For received signals, breathing signal and noise cannot be separated directly, thus we utilize the power spectral density (PSD) to estimate SNR. More concretely, we estimate SNR by the ration of signal energy within the range of normal respiratory rate to signal energy beyond normal respiratory rate. Then the weight of each subcarrier can be calculated according to the SNR using MRC method. We multiply each subcarrier by its corresponding weight and add them to combine all subcarriers. In this way, the combined signal with maximum SNR can be obtained by using MRC.

Fig. 9 depicts an illustrative example of MRC method for breathing signal maximization based on real-world measurements. Subcarrier (SC) #12 has the highest SNR compared to other subcarriers, which contributes the most to the combined signal, while subcarrier #30 with minimum SNR makes contributes the least to the combined signal. Other subcarriers also make corresponding contribution to the final combined signal. As shown in Fig. 9(c), all subcarriers are combined into one. We can see from this figure that MRC largely enhances the respiratory signal and the respiration waveform by using MRC is consistent with the ground truth from the respiratory sensor.

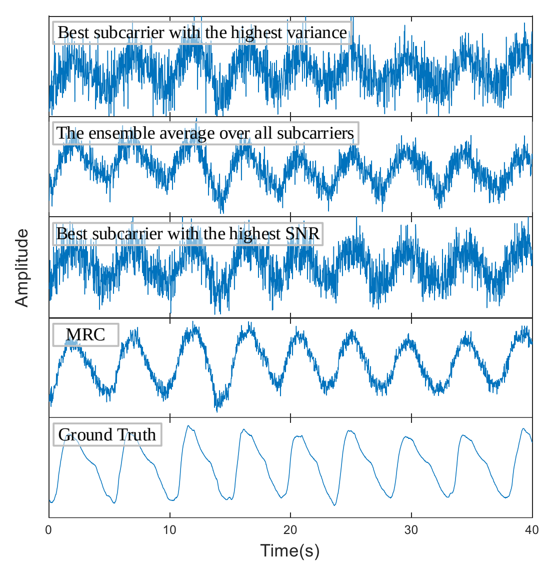

Fig. 10. Comparison of respiratory signal using four different methods.

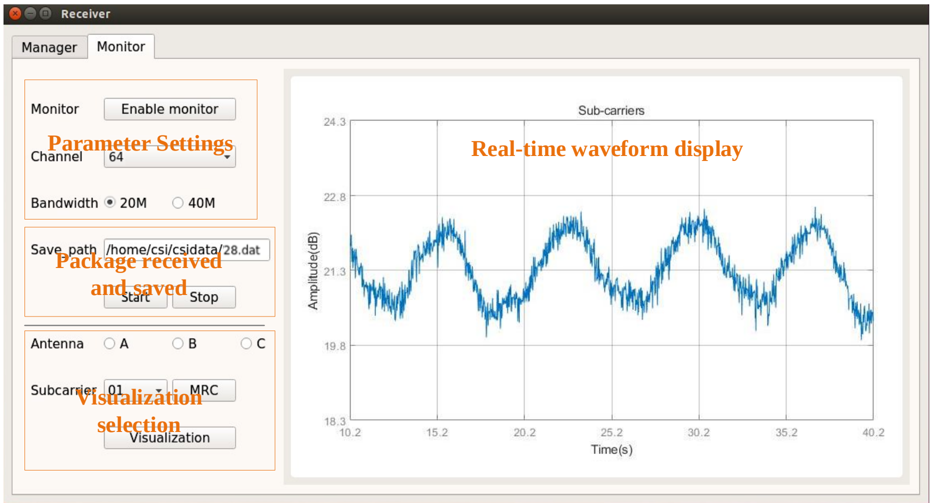

Fig. 11. Real-time display interface.

We compare four different methods of signal enhancement: selecting the best subcarrier with the highest variance, the ensemble average over all subcarriers, selecting the best subcarrier with the highest SNR, and MRC. The result of comparison is shown in Fig. 10. As seen, no matter what selection criteria is used, any single subcarrier is not the optimal estimation. The respiratory signals on different subcarriers cannot be averaged directly, which may cancel respiratory signals. MRC considers the SNR on different subcarriers, and the combined respiration waveform by MRC has a better effect than the other methods.

For the amplitude information of each exercise training, we obtain the clear and genuine waveforms after outlier removal and MRC method. We implement a real-time processing program using Qt Creator to display the waveforms directly output, as shown in Fig.11. The visualized graphic display can provide a visual feedback for the patient.

In the rehabilitation exercise training, the activity of the patient is continuous, and different human activities have different disturbance effects on the wireless signal so that the received waveforms are different. Based on these observations, we propose an activity segmentation method based on state transition difference, which uses amplitude variance change to segment automatically all processes of rehabilitation exercise training in the continuously collected WCI measurements.

C. *Exercise Assessment*

The exercise assessment aims to characterize the quality of rehabilitation exercises and provides feedbacks to the patient and doctors. In order to measure the quality, we first extract valuable information from each rehabilitation exercise and then analyze the changes in rehabilitation exercise by integrating this information. Specifically, we assess the quality of rehabilitation exercise by focusing on its duration, intensity, and breathing changes.

1) *Duration*

Duration is how long a person performs an exercise session. The duration of exercise is an essential factor affecting the effect of rehabilitation training. Hence extracting exercise duration from collected wireless signals is crucial to assess the quality of rehabilitation training. We first calculate the time of each conducted exercise from collected WCI measurements. We then add these times together to get the duration of a rehabilitation exercise training. By combining the duration of each rehabilitation training in chronological order, the changing trend of duration can be obtained.

2) *Intensity*

Exercise intensity depicts how hard a person's body is working during exercise, which is another important factor for evaluating the quality of rehabilitation exercises. So it is significant for tracking the patient's rehabilitation process to extract exercise intensity from received WCI measurements. In this paper, for aerobic exercise we propose speed to characterize exercise intensity, and for strength training we use the number of repetitions of the movements to describe exercise intensity. Comparing the variation of exercise intensity over time can keep better track the patient's exercise status.

3) *Breathing Changes*

Breathing Changes are mainly in view of breathing exercises and refer to changes in respiratory rate and depth. The control of breathing depth and rate is an effective strategy for restoring and enhancing respiratory function. In breathing exercises, we consciously alter our breathing rate and depth but do not know what the changes are. If the breathing changes are known, the patient can better perform breathing exercises. Hence, we need to acquire respiratory rate and depth from the measured respiration waveforms. Specifically, let T_i and T_e denote the inspiratory time and the expiratory time respectively, then the instantaneous respiratory rate (IRR) is expressed as

$$IRR = \frac{1}{T_i + T_e} \, (Unit\text{: } Hz) \tag{7}$$

Let A_p and A_t represent the amplitude value of the crest and the trough in respiration waveforms respectively, then the change of respiratory depth (CRD) is denoted as

$$CRD = A_p - A_t \tag{8}$$

V. Evaluation

In this section, we conduct extensive experiments and evaluate the performance of EMAS in monitoring and assessing rehabilitation exercise training.

A. Experiment Setup

We implement EMAS using the designed compact and portable prototype, which are equipped with off-the-shelf network adapter and built-in batteries for rapid real-world deployment. The prototype run Linux with the 4.8.2 kernel. Our system consists of two prototypes, one as the transmitter and the other as the receiver. Both operate at 5.32 GHz band with a bandwidth of 20 MHz. The transmitter sends data packets at a rate of 50 Hz and the receiver captures theses data packets.

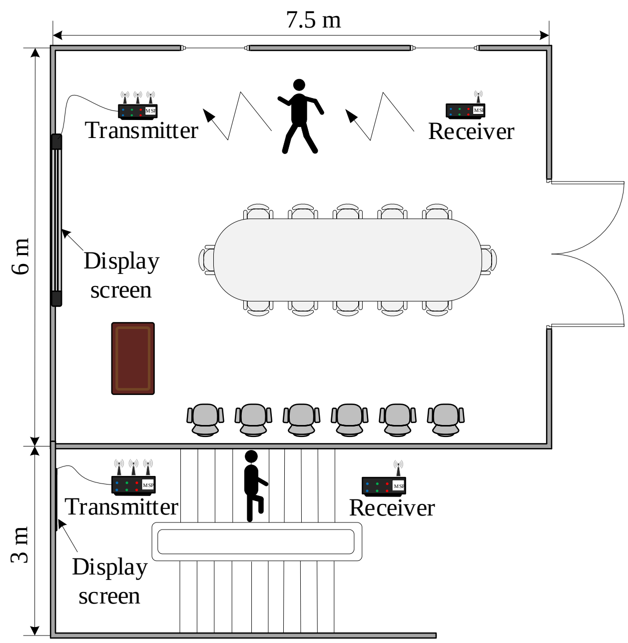

Fig. 12. Experiment settings for rehabilitation exercise monitoring.

We carry out experiments by deploying EMAS in a conference room and the stairs next to it, as depicted in Fig.12. We consider different settings by placing the transmitter and receiver at different locations during diverse rehabilitation exercises. In brisk walking, the transmitter and receiver are 5 m apart, and the height of them is 0.7 m. In stair climbing, the transmitter and receiver are separated by 11 stair-steps, with a height of 0.7 m. In strength training, the distance between the transmitter and receiver is also 5 m, and the height is 1.2 m. In breathing exercises, the transmitter and receiver are placed roughly 2 m apart, and their height is parallel to the abdomen. We collect one week of exercise data from four subjects aged from 23 to 28, of which two are female, and two are male. Each subject signs an informed consent before participating. All subjects are asked to carry out rehabilitation exercises with five times during one week. A complete rehabilitation exercise program includes three things: aerobic exercise (a 30-minute exercise program of brisk walking or a 30-minute exercise program of stair climbing), strength training (front raise and lateral raise), and breathing exercises (abdominal breathing and pursed-lip breathing).

To obtain the ground truth, videos are taken to simultaneously record the experiments in aerobic exercise and strength training and a contact respiratory sensor is used to collect respiratory data simultaneously in breathing exercises. The respiratory sensor (HKH-11C) utilize the piezoelectric effort to measure the movement of abdomen due to breathing. Its sampling rate is 50 Hz, same as EMAS.

B. Evaluation

1) Evaluation on Exercise Monitoring

We evaluate the performance of EMAS for exercise monitoring by comparing its results with the ground truth.

For aerobic exercise, one male subject and one female subject are asked to carry out the 30-minute exercise program of brisk walking, and another male and female are asked to carry out the 30-minute exercise program of stair climbing. Brisk walking requires the subject walk back and forth as fast as possible in a 5m-long straight. Stair climbing asks the subject to walk up and down a flight of stairs with 11 steps.

Fig. 13(a) shows a fragment of the monitoring result when a subject performed a 30-minute exercise program of brisk walking. Comparing the waveform of brisk walking with corresponding video streams, we observe that the waveform generates the change of ellipse labeling in Fig. 13(a) when the subject took a brisk walk back and forth. Further comparison shows that there are a few seconds to prepare before beginning exercise because the subject has to press the “Start” button on the receiver. We can also see that the amplitude fluctuations caused by limb movements during the preparation and during the break is much smaller than the amplitude fluctuations caused by whole body movements during brisk walking. Therefore, we employ the proposed activity segmentation method based on state transition difference to detect easily the process of brisk walking from all the collected measurements. We then use the peak detection algorithm to detect the number of walking laps by setting the appropriate thresholds. Due to the amplitude difference of different subjects, the normalization is carried out before using the peak detection algorithm. In Fig. 13(a), the subject walked 43.5 laps during first five-minute brisk walking and then rested for about a minute, which is a cycle. The 30-minute exercise program of brisk walking includes five such cycles.

Fig. 13(b) shows the 7-min amplitude measurements extracted from a subject’s 30-minute exercise program of stair climbing. Compared with the videos, when the subject climbed stairs one time, the waveform of stair climbing produced the change of ellipse labeling in Fig. 13(b), which is obviously different from the waveform change of brisk walking. Comparison of the result of stair climbing and brisk walking indicates that the waveforms of the two kind of exercise were obviously different and difference in velocity between the two. As can be seen from Fig. 13(b), the subject walked up and down stairs 26 times during five-minute stair climbing, much less than brisk walking.

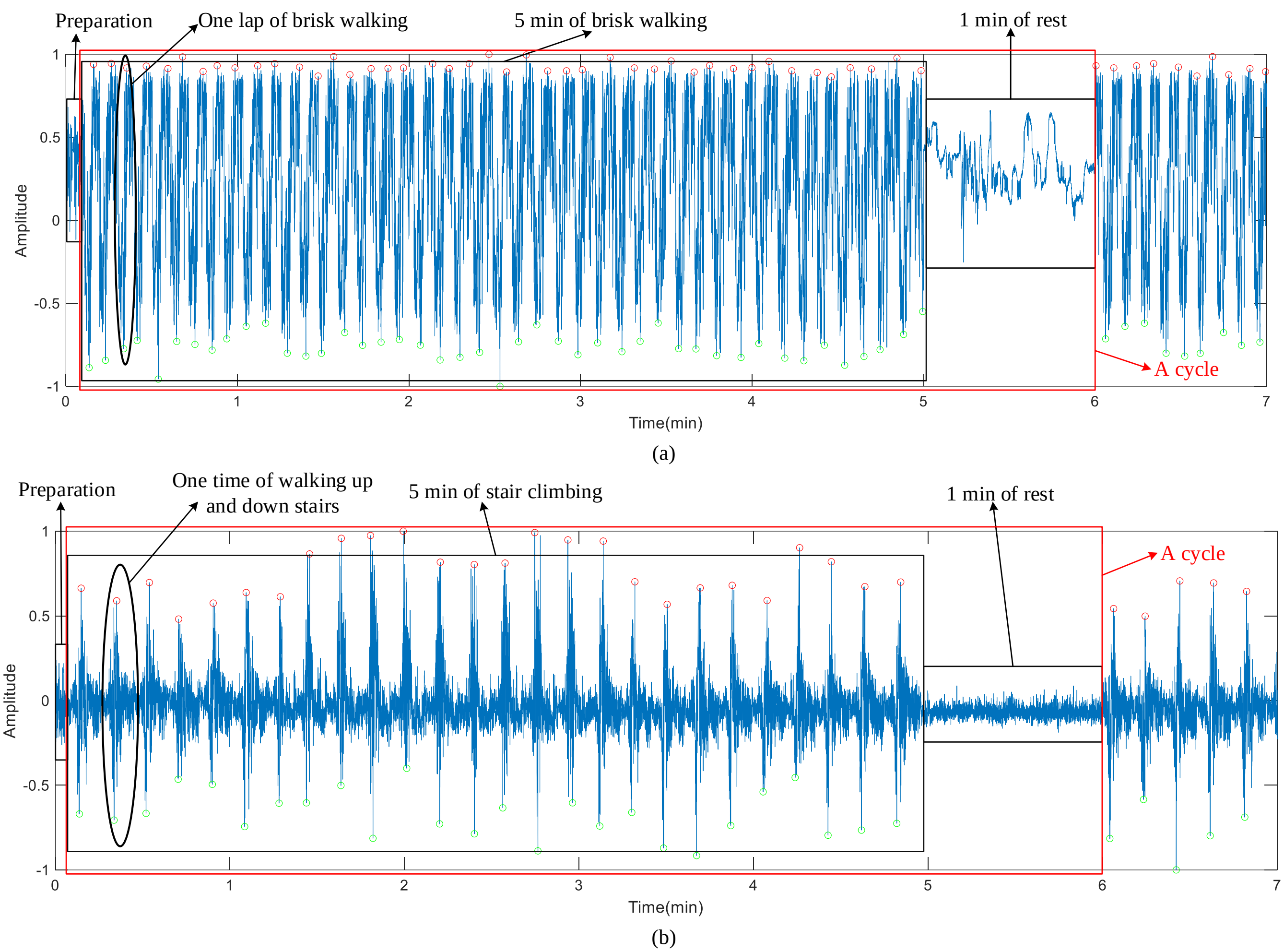

Fig. 13. The 7-min amplitude measurements extracted from a subject's 30-minute exercise program of (a) brisk walking and (b) stair climbing.

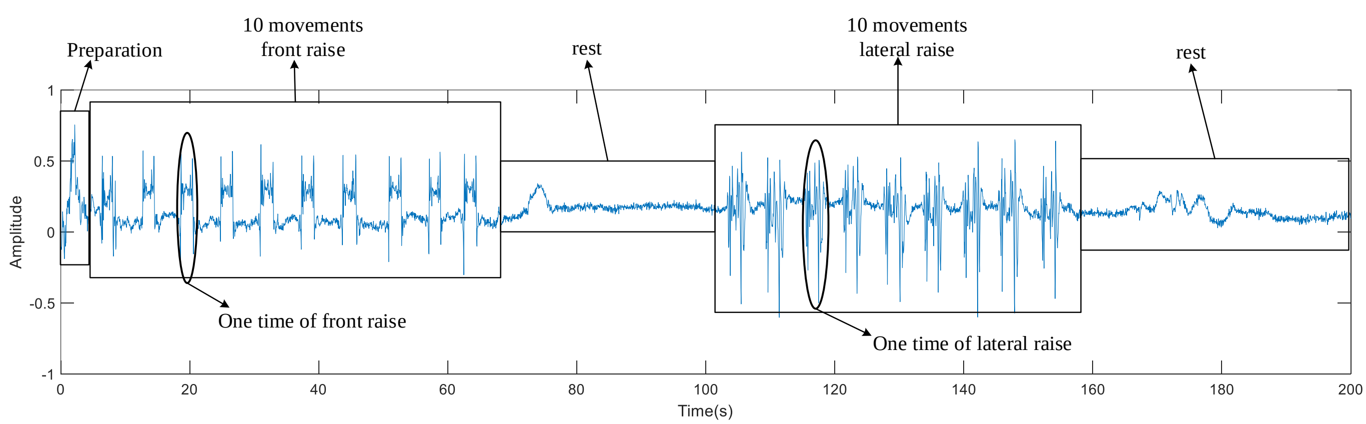

Fig. 14. A set of the monitoring result when a subject performed exercise program of strength training.

For strength training, we ask subjects to choose a set of weight dumbbells that suited themselves and complete the designed exercise program of strength training. Here we also use the activity segmentation method based on state transition difference to segment the strength training processes and the peak detection algorithm to detect the number of repetitions of the movements by setting the appropriate thresholds. Fig. 14 shows one set of the monitoring result from a subject's exercise program of strength training. Compared with the video streams, the waveform changes caused by front raise and lateral raise were different, and this set of strength training contained 10 reps of front raise, 10 reps of lateral raise, and 2 short breaks. It is evident from Fig. 14 that the amplitude fluctuations caused by repetitive movements have good repeatability and the amplitude fluctuations caused by different movements have obvious difference. The result shows that EMAS could precisely monitor the proposed aerobic exercises and strength training.

For breathing exercises, the subject needs doing abdominal breathing and pursed-lip breathing. Abdominal breathing requires a person to breathe in slowly through the nose and feel the abdomen rise, and then breathe out slowly through the mouth and let the abdomen fall downward, making breath slow, deep and regular. Pursed-lip breathing requires a person to inspire through the nose with the mouth closed and exhale through lips having a pursed appearance at a slow controlled flow, breathe out for twice as long as breathe in. During the experiments, the subject is asked to sit on a chair quietly, and place one hand on chest and one on abdomen.

We evaluate the respiratory monitoring accuracy of EMAS by comparing EMAS with the respiratory sensor. The respiratory sensor is attached to the subject's abdomen as the ground truth. The normalized wireless signals and respiratory sensor signals are shown in Fig. 15. Note that the wireless signals are filtered by using the Hampel identifier and MRC method. We can see from Fig. 15 that for abdominal breathing and pursed-lip breathing EMAS-detected signals gives the good correlation to the respiratory sensor-detected one. The result demonstrates EMAS as a non-contact method has ability to precisely monitoring the respiratory movements.

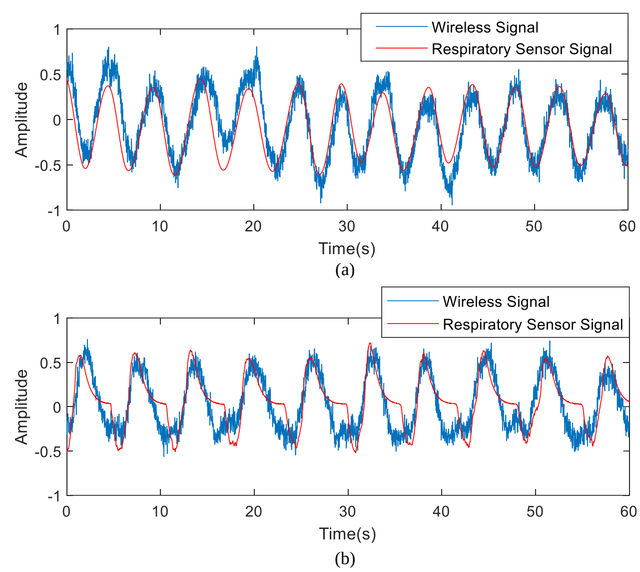

Fig. 15. The normalized wireless signals and respiratory sensor signals of (a) abdominal breathing and (b) pursed-lip breathing.

2) *Evaluation on Exercise Assessment*

To evaluate the effectiveness of EMAS for exercise assessment, we analyze the exercise data of four subjects for a week form the perspectives of duration, intensity and breathing changes.

Exercise duration can be calculated using the received WCI data packets. Each received packet includes a timestamp. For a complete rehabilitation exercise program, we first calculate the duration of aerobic exercise, strength training and breathing exercises separately based on the timestamps of the corresponding packets, and then add these three durations to acquire the duration of the rehabilitation exercise. Fig. 16 depicts that the duration of a subject's rehabilitation exercise five times in one week, including the duration of various exercise programs and the overall duration of rehabilitation exercise. It can be seen that the overall duration of each rehabilitation exercise is nearly constant at about one hour.

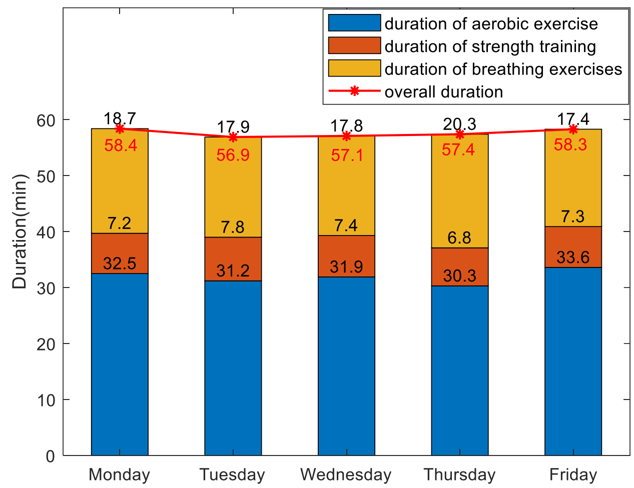

Fig. 16. The duration of a subject's rehabilitation exercise in one week.

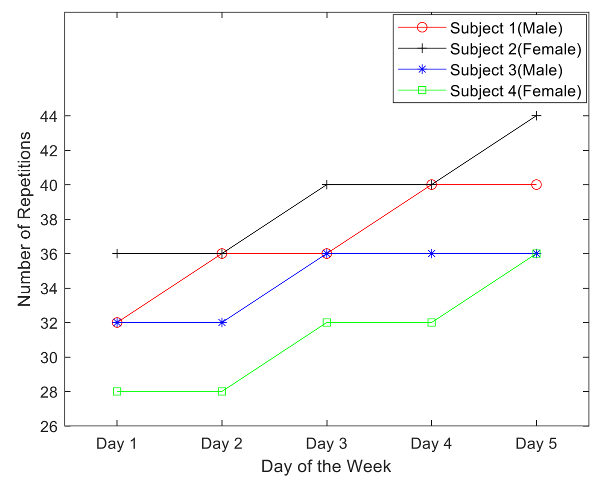

Fig. 17. Number of repetitions per strength training in one week.

Exercise intensity is an important indicator for assessment of aerobic exercise and strength training. In this paper, exercise intensity is measured by brisk-walking speed in brisk walking, stair-climbing speed in stair climbing, and the number of repetitions of the movements in strength training. We first estimate the distance of brisk walking by multiplying the number of walking laps by 10 m (the distance of a lap is considered as 10 m) and then calculate the time by the timestamp corresponding to the process of brisk walking, to get the brisk-walking speed. We also use the same approach to get the stair-climbing speed (One time of walking up and down the stairs is 22 steps with a step height of 15 cm). The brisk-walking speed and the stair-climbing speed of all subjects for one week are summarized in Table I. It can be seen form Table I that: 1) each subject's speed is basically stable during aerobic exercise in a week; 2) Men walk faster than women during the brisk walking and stair climbing; 3) the speed and intensity selected by these subjects meets recommendations for moderate intensity exercise according to the current studies [44, 45].

TABLE I
BRISK-WALKING SPEED AND STAIR-CLIMBING SPEED OF ALL SUBJECTS

	Brisk-walking Speed $(\mathrm{m \cdot s^{-1}})$					Stair-climbing Speed $(\mathrm{m \cdot s^{-1}})$				
	Day 1	Day 2	Day 3	Day 4	Day 5	Day 1	Day 2	Day 3	Day 4	Day 5
Subject 1(Male)	1.59	1.54	1.53	1.56	1.57	/	/	/	/	/
Subject 2(Female)	1.46	1.36	1.42	1.46	1.47	/	/	/	/	/
Subject 3(Male)	/	/	/	/	/	0.31	0.29	0.30	0.31	0.32
Subject 4(Female)	/	/	/	/	/	0.28	0.25	0.24	0.26	0.27

Furthermore, we extract the number of repetitions of the movements per strength training to characterize the strength training intensity, as shown in Fig. 17. The observation we can make from this figure is that all subjects' exercise intensity shows an upward trend with the increase of exercise times. Note that the intensity of strength training is also related to by dumbbell weights. Dumbbell weight used by each subject is unchanging during this week of strength training.

IRR and CRD are used to describe breathing changes during breathing exercises in this paper. We use an improved peak detection algorithm to pinpoint the crests and the troughs of respiratory waveforms. Two key improvements to the algorithm are: 1) set a threshold on the minimum distance between two consecutive peaks according to human respiratory rate; 2) the amplitude change between the wave trough and its subsequent 25th interval point (equivalent to 0.5 s) should be greater than 1 dB in pursed-lip breathing. Fig. 18 shows the detection results of a subject's abdominal breathing and pursed-lip breathing using the improved peak detection algorithm, which indicates that using this algorithm can accurately identify the crests and the troughs of respiratory waveforms in in two types of breathing exercises. We then calculate IRR and CRD from the detected crests and troughs. As shown in Fig. 18(a), for abdominal breathing we compute the inspiratory time T_i of 2.78 s, the expiratory time T_e of 2.80 s in a respiratory cycle based on the detected crests and troughs, thus obtaining IRR of 0.18 Hz. And in this respiratory cycle CRD for inspiration and expiration are 3.30 dB and 3.40 dB. Overall, the average respiratory rate is 0.17 Hz, the change of respiratory depth is about 3 to 4 dB, and the inspiration-to-expiration ratio (I: E) is 1:1. Similarly, from Fig. 18(b) in pursed-lip breathing the inspiratory time T_i and the expiratory time T_e of a respiratory cycle is 1.90 s and 3.72 s, thus IRR is calculated as 0.18 Hz. And CRD of inspiration and expiration are 4.37 dB and 5.28 dB respectively in this respiratory cycle. As a whole, for pursed-lip breathing the average respiratory rate is 0.16 Hz, the change of respiratory depth is about 3 to 5 dB, and I: E is 1:2.

We use the above approaches to extract exercise information of all subjects and further assess this information, and the assessment results are fed back to all subjects. Note that all participant in the experiment are healthy subjects. The proposed EMAS would undergo extensive clinical trials on real patients with respiratory diseases in future work, making it available to the patients for home-based respiratory rehabilitation.

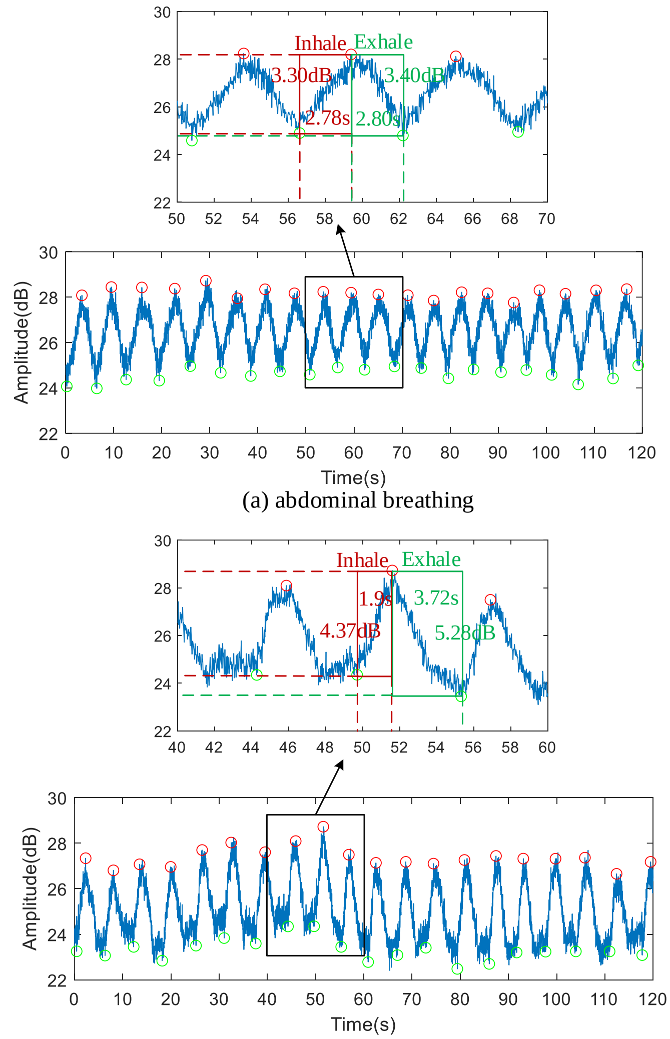

(a) abdominal breathing

(b) pursed-lip breathing

Fig. 18. Breathing changes extracted from a subject's (a) abdominal breathing and (b) pursed-lip breathing.

VI. CONCLUSION

In this paper, we present the design, implementation, and evaluation of EMAS, a non-contact exercise monitoring and assessment system using WiFi-based multi-band microwave sensing technique. The key novelty of EMAS is to monitor in real-time and assess accurately home-based exercise training for respiratory rehabilitation using ubiquitous WiFi signals. EMAS can not only provide an online visual feedback during the execution of exercise training, but also extract exercise duration, exercise intensity and breathing changes to assess the performance of rehabilitation exercise training. To achieve this, a series of signal processing techniques are proposed to obtain optimal waveforms and extract from it useful exercise information. In addition, the designed prototype of EMAS is compact, portable, low-cost and user-friendly, which can be applied in real scenarios for home-based exercise monitoring in daily life. We believe that EMAS is a promising step towards practical wireless home-based exercise training monitoring.

References

[1] M. A. Spruit et al., "An official American Thoracic Society/European Respiratory Society statement: key concepts and advances in pulmonary rehabilitation," *American journal of respiratory and critical care medicine*, 188.8 (2013): e13-e64.

[2] L. L. Y. Tsai et al., "Home-based telerehabilitation via real-ime videoconferencing improves endurance exercise capacity in patients with COPD: the randomized controlled TeleR Study," *Respirology*, 22.4 (2017): 699-707.

[3] N. Charususin et al., "Randomised controlled trial of adjunctive inspiratory muscle training for patients with COPD," *Thorax*, 73.10 (2018): 942-950.

[4] COPD Working Group, "Pulmonary rehabilitation for patients with chronic pulmonary disease (COPD): an evidence-based analysis," *Ontario Health Technology Assessment* Ser., Vol. 12: No. 6(2012):1-75.

[5] C. S. Gordon et al., "Effect of pulmonary rehabilitation on symptoms of anxiety and depression in COPD: a systematic review and meta-analysis," *Chest*, 156.1 (2019): 80-91.

[6] P. Goyal et al., "Clinical characteristics of COVID-19 in New York City," *New England Journal of Medicine*, 382.24(2020).

[7] C. Huang et al., "Clinical features of patients infected with 2019 novel coronavirus in Wuhan, China," *The Lance*t, 395.10223(2020).

[8] V. Surveillances, "The epidemiological characteristics of an outbreak of 2019 novel coronavirus diseases (COVID-19)—China, 2020," *China CDC weekly*, 2.8 (2020): 113-122.

[9] L. E. Osborn et al., "Sensing and Control for Prosthetic Hands in Clinical and Research Applications," *Wearable Robotics. Academic Press*, pp. 445–468, 2020.

[10] D. Burns et al., "Shoulder Physiotherapy Exercise Recognition: Machine Learning the Inertial Signals from a Smartwatch," *Physiological Measurement*, 39.7(2018):075007 (9pp).

[11] L. Bavan et al., "Adherence Monitoring of Rehabilitation Exercise with Inertial Sensors: A Clinical Validation Study," *Gait & Posture*, 70(2019):211-217.

[12] G. Nguyen et al., "Quantification of Compensatory Torso Motion in Post-Stroke Patients Using Wearable Inertial Measurement Units." *IEEE Sensors Journal* 21.13 (2021): 15349-15360.

[13] M. Panwar et al., "Rehab-net: Deep learning framework for arm movement classification using wearable sensors for stroke rehabilitation," *IEEE Transactions on Biomedical Engineering*, 66.11 (2019): 3026-3037.

[14] C. N. Teague et al., "A wearable, multimodal sensing system to monitor knee joint health." *IEEE Sensors Journal* 20.18 (2020): 10323-10334.

[15] Y. Zhou et al., "sEMG bias-driven functional electrical stimulation system for upper-limb stroke rehabilitation." *IEEE Sensors Journal* 18.16 (2018): 6812-6821.

[16] Z. Zhang, "Microsoft Kinect Sensor and Its Effect," *IEEE Multimedia*, 19.2 (2012):4-10.

[17] X. Yu and S. Xiong. "A Dynamic Time Warping Based Algorithm to Evaluate Kinect-Enabled Home-Based Physical Rehabilitation Exercises for Older People." *Sensors*, 19.13 (2019):2882.

[18] M. Idoudi et al., "Wireless visual sensor network platform for indoor localization and tracking of a patient for rehabilitation task." *IEEE Sensors Journal* 18.14 (2018): 5915-5928.

[19] B. Bruno et al., "3D Analysis of Upper Limbs Motion during Rehabilitation Exercises Using the Kinect™ Sensor: Development, Laboratory Validation and Clinical Application," Sensors, 18.7 (2018): 2216.

[20] F. Mortazavi et al, "Continues online exercise monitoring and assessment system with visual guidance feedback for stroke rehabilitation," *Multimedia Tools and Applications*, 78.22 (2019): 32055-32085.

[21] C. Uysal et al., "RF-Wri: An efficient framework for RF-based device-free air-writing recognition." *IEEE Sensors Journal* 21.16 (2021): 17906-17916.

[22] M. Zhao et al., "RF-based 3D skeletons." *Proceedings of the 2018 Conference of the ACM Special Interest Group on Data Communication*. 2018.

[23] J. Lien et al., "Soli: Ubiquitous gesture sensing with millimeter wave radar," *ACM Transactions on Graphics (TOG)*, 35.4 (2016): 1-19.

[24] X. Liu et al., "Kalman filter-based data fusion of wi-fi rtt and pdr for indoor localization." *IEEE Sensors Journal* 21.6 (2021): 8479-8490.

[25] X. Li et al., "Dynamic-music: accurate device-free indoor localization," *Proceedings of the 2016 ACM International Joint Conference on Pervasive and Ubiquitous Computing*. 2016.

[26] W. Wang et al., "Device-free human activity recognition using commercial WiFi devices," *IEEE Journal on Selected Areas in Communications*, 35.5 (2017): 1118-1131.

[27] H. Zou et al., "Deepsense: Device-free human activity recognition via autoencoder long-term recurrent convolutional network," *2018 IEEE International Conference on Communications (ICC)*. IEEE, 2018.

[28] S. Duan et al., "Widriver: Driver activity recognition system based on wifi csi," *International Journal of Wireless Information Networks*, 25.2 (2018): 146-156.

[29] K. Ali et al., "Recognizing keystrokes using WiFi devices." *IEEE Journal on Selected Areas in Communications*, 35.5 (2017): 1175-1190.

[30] G. Wang et al., "We can hear you with Wi-Fi!" *IEEE Transactions on Mobile Computing*, 15.11 (2016): 2907-2920.

[31] X. Wang et al., "Resilient respiration rate monitoring with realtime bimodal CSI data." *IEEE Sensors Journal* 20.17 (2020): 10187-10198.

[32] X. Yang et al., "Wandering pattern sensing at S-band," *IEEE journal of biomedical and health informatics*, 22.6 (2017): 1863-1870.

[33] D. Fan et al., "Small-Scale Perception in Medical Body Area Networks," *IEEE journal of translational engineering in health and medicine*, 7 (2019): 1-11.

[34] J. Ding et al., "Multimodal Fusion-AdaBoost Based Activity Recognition for Smart Home on WiFi Platform." *IEEE Sensors Journal* 22.5 (2022): 4661-4674.

[35] J. Su et al., "Human Activity Recognition Using Self-powered Sensors Based on Multilayer Bi-directional Long Short-Term Memory Networks." *IEEE Sensors Journal* (2022).

[36] Y. Wang et al., "Robust CSI-based human activity recognition with augment few shot learning." *IEEE Sensors Journal* 21.21 (2021): 24297-24308.

[37] M. Speth et al., "Optimum receiver design for wireless broad-band systems using OFDM. I," *IEEE Transactions on Communications*, vol. 47, no. 11, pp. 1668–1677, Nov. 1999.

[38] C. Jacome et al., "Pulmonary Rehabilitation for Mild COPD: A Systematic Review," *Respiratory Care*, 59.4 (2014): 588-594.

[39] L. Yang et al., "Pulmonary rehabilitation for patients with coronavirus disease 2019 (COVID-19)," *Chronic diseases and translational medicine*, 6.02 (2020): 79-86.

[40] A. Gugnani et al., "Effect of Diaphragmatic Breathing and Pursed Lip Breathing In Improving Dyspnea-A Review Study," *European Journal of Molecular & Clinical Medicine*, 7.6 (2020): 2643-2646.

[41] Nguyen JD, Duong H. Pursed-lip Breathing. [Updated 2020 Aug 11]. In: StatPearls [Internet]. Treasure Island (FL): StatPearls Publishing; 2021 Jan-. Available from: https://www.ncbi.nlm.nih.gov/books/NBK545289/

[42] L. Davies et al., "The identification of multiple outliers," *Journal of the American Statistical Association*, 88.423 (1993): 782-792.

[43] J. R. Barry, E. A. Lee, and D. G. Messerschmitt, "Digital Communication," 2004, doi: 10.1007/978-1-4615-0227-2.

[44] E. M. Murtagh et al., "Speed and Exercise Intensity of Recreational Walkers," *Preventive Medicine*, 35.4 (2002): 397-400.

[45] E. Michae et al., "Home-Based Stair Climbing as an Intervention for Disease Risk in Adult Females: A Controlled Study," *International Journal of Environmental Research and Public Health*, 18.2 (2021): 603.